Research Article | Vol. 29, No. 3 / 1 February 2021 / Optics Express 3258
Optics EXPRESS

InGaN-diode-pumped AlGaInP VECSEL with sub-kHz linewidth at 689 nm

PAULO H. MORIYA,[1,*] RICCARDO CASULA,[1] GEORGE A. CHAPPELL,[1] DANIELE C. PARROTTA,[1,3] SANNA RANTA,[2] HERMANN KAHLE,[2] MIRCEA GUINA,[2] AND JENNIFER E. HASTIE[1]

[1]*Institute of Photonics, Department of Physics, SUPA, University of Strathclyde, The Technology and Innovation Centre, 99 George Street, Glasgow G1 1RD, UK*
[2]*Optoelectronics Research Centre, Physics Unit / Photonics, Tampere University, Korkeakoulunkatu 3, 337201 Tampere, Finland*
[3]*Now at Coherent Scotland Ltd, West of Scotland Science Park, Maryhill Rd. Glasgow G20 0XA, UK*
[*]*paulo.moriya@strath.ac.uk*

Abstract: We report the design, growth, and characterization of an AlGaInP-based VECSEL, designed to be optically-pumped with an inexpensive high power blue InGaN diode laser, for emission around 689 nm. Up to 140 mW output power is achieved in a circularly-symmetric single transverse (TEM_{00}) and single longitudinal mode, tunable from 683 to 693 nm. With intensity stabilization of the pump diode and frequency-stabilization of the VECSEL resonator to a reference cavity via the Pound-Drever-Hall technique, we measure the power spectral density of the VECSEL frequency noise, reporting sub-kHz linewidth at 689 nm. The VECSEL relative intensity noise (RIN) is <-130 dBc/Hz for all frequencies above 100 kHz. This compact laser system is suitable for use in quantum technologies, particularly those based on laser-cooled and trapped strontium atoms.

1. Introduction

Many quantum technology systems, particularly those based on cold atoms, are dependent on multiple laser sources to manipulate atoms, addressing numerous transitions at optical frequencies. The development of more compact and portable laser systems with performance similar or superior to current laser solutions in terms of overall stability, brightness and narrow linewidth operation is crucial to the advancement and miniaturization of quantum technologies for applications outside the laboratory environment. This is a particular challenge when ultra-narrow atomic transitions at novel wavelengths are targeted [1–3], as for example the neutral strontium cooling and clock transitions at 689 and 698 nm, respectively [4]. In the past decade, optically-pumped vertical-external-cavity surface-emitting lasers (VECSELs) [5,6] have achieved higher brightness and narrower intrinsic linewidth operation when compared to other semiconductor laser technologies from the ultra-violet to the infra-red, via direct emission or efficient intra-cavity nonlinear conversion [7–12], with potential for miniaturization. With the exception of the shorter wavelength systems, the multi-quantum well gain structures of VECSELs are most often pumped using low brightness diode lasers and arrays, especially for emission wavelengths between 900 and 1200 nm (e.g., using InGaAs quantum wells) where high power and low cost 808 nm diodes are widely available. Almost all the pump light is absorbed within the first couple of microns in the vertical semiconductor structure such that complex pump beam shaping is not required. This can facilitate very compact integration of the pump with the laser system packaging (see e.g. [13]). Targeting shorter (visible) fundamental wavelength emission, on

#416210 https://doi.org/10.1364/OE.416210
Journal © 2021 Received 27 Nov 2020; revised 21 Dec 2020; accepted 21 Dec 2020; published 19 Jan 2021

Optics EXPRESS

the other hand, usually requires less efficient visible pumps, such as solid-state lasers [14], dye lasers [15], or even frequency-doubled IR VECSELs [16], thus increasing the total volume. For example, GaInP/AlGaInP, AlGaAs/AlGaInP, and GaInAsP/AlGaInP quantum well VECSELs with emission between 630 and 830 nm have been extensively studied when barrier-pumped at 532 nm [17–19], or in-well pumped at 640 nm [20].

The emergence of InGaN diode lasers [21] with emission at blue wavelengths (44X–46X nm) in the early 2000s, enabled a preliminary demonstration of diode-pumping of an AlGaInP-based VECSEL [22]. Here the gain region and the distribution of GaInP quantum wells (QWs) had to be shortened in comparison to the previous green-pumped material: at green wavelengths, the quaternary semiconductor AlGaInP has absorption coefficient $\alpha_{532} \approx 2.4 \times 10^4$ cm^{-1} [23,24] resulting in an absorption length >1-μm and a corresponding 5λ-long gain region where 10–20 quantum wells (QWs) can be distributed over 10 optical field anti-nodes for resonant periodic gain (RPG) [25]. At blue wavelengths (44X–45X nm), however, the absorption coefficient of the material increases significantly to $\alpha_{445} \approx 9.5 \times 10^4$ cm^{-1} [23,24], thus reducing the length of the gain region before pump depletion, and thus the number of available field antinodes to 2 or 3. As described in Smith's paper the quantum wells were distributed asymmetrically in a 4–3 configuration in the first two anti-nodes of the optical standing wave, resulting in laser emission at 672 nm with output power of 12.2 mW, limited by the available pump power of 500 mW [22]. Since this initial work the development and commercialization of multi-mode InGaN diode lasers has rapidly progressed, driven by numerous applications including material processing [26], communications [27] and lighting [28], such that low cost devices composed of multiple emitters mounted in TO-5 and TO-9 cans are now available with output powers of several W [29].

In our recent work we have developed ultra-narrow linewidth AlGaInP-based VECSELs emitting at 689 nm [16], demonstrating, for the first time with this laser type, the sub-kHz linewidths required for targeting the second cooling transition of neutral strontium [30]. However, these results were obtained by pumping with a high brightness, low noise green pump (a frequency-doubled IR VECSEL), such that further reductions in the size, weight, power, and cost (SWaP-C) of the system require the implementation of inexpensive diode-pumping. This not only requires a re-design of the multi-QW gain region, as explained above, but effective management of the associated increase in noise injected into the VECSEL by these lasers. The pump intensity noise is directly transferred to the VECSEL as an intensity modulation, and further, carrier- and thermally-induced index fluctuations in the gain structure that lead to cavity length fluctuations, and thus increased frequency noise [31–33]. These noise contributions occur in frequency bands below the VECSEL cavity cut-off (up to a few MHz, depending on cavity length and finesse), which results in linewidth broadening orders of magnitude greater than the fundamental (or Schawlow-Townes-Henry) limit [34,35].

In this paper, we present the results of InGaN-diode-pumping of an AlGaInP-based VECSEL system designed for strontium cooling, achieving >140 mW single frequency output at the target wavelength of 689 nm, representing an order of magnitude increase in power compared with previous work [22]. We describe the design and growth of the new gain structure, and the design of the high power pump system based on an inexpensive InGaN diode laser (TO-5 can), including temperature, current, and intensity stabilization. Finally, we present the characterization of the pump and VECSEL laser performance, including measurements of the relative intensity noise (RIN) of both lasers and the power spectral density of the VECSEL frequency noise relative to a commercial reference cavity. Sub-kHz linewidth (~0.6 kHz) is inferred from the latter, achieved with simultaneous active stabilization of the pump intensity, via the diode current, and the VECSEL resonator, via the Pound-Drever-Hall technique.

Optics EXPRESS

2. Gain structure design and growth

To target longer wavelengths at 689 nm when optically-pumped at wavelengths around 450 nm we used a VECSEL gain structure with highly-compressively-strained GaInP QWs, distributed to match the short absorption length at this pump wavelength (see Fig. 1). In this scenario, assuming low mobility of the carriers generated in the barrier material [36,37], all the QWs are placed close to the semiconductor surface which, in order to maintain RPG, results in a larger number of QWs per antinode. The design presented here includes 8 GaInP QWs, each with a thickness of 8-nm, positioned for RPG in an asymmetrical 4-3-1 distribution over the first 3 antinodes of the optical field formed inside the semiconductor sub-cavity. The QW barriers (shown in orange) are tensile-strained to compensate the compressively-strained QWs (yellow), while the region between the 2nd and 3rd antinodes (blue) is lattice-matched. The gain region is enclosed by high bandgap, lattice-matched confinement windows (purple). The full gain structure was grown on a 2" diameter GaAs substrate by molecular beam epitaxy (MBE) on top of a distributed Bragg reflector (DBR) consisting of 35.5 pairs of AlGaAs/AlAs quarter-wave layers with reflectivity >99.98% at 689 nm. After growth the wafer was treated with rapid thermal annealing, performed at 700 ± 30 °C for 300 s, to reduce defects in the QWs [38].

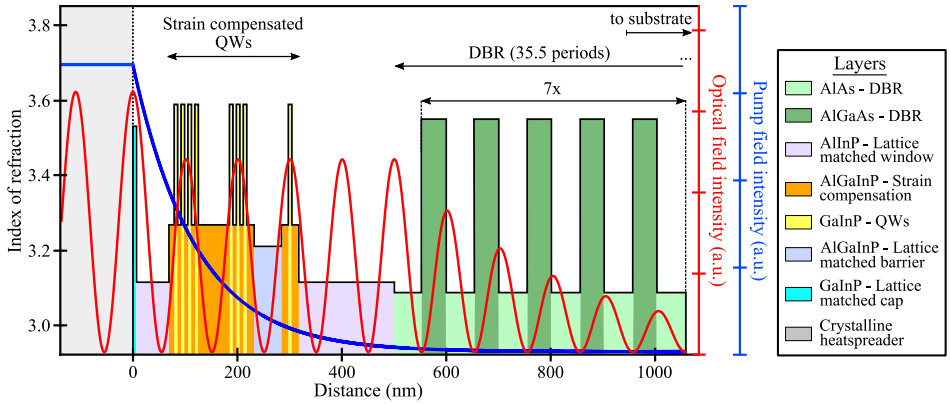

Fig. 1. Schematic of the AlGaInP VECSEL gain structure designed for emission at 689 nm under optical pumping at wavelengths around 450 nm with an asymmetrical distribution of quantum-wells.

3. InGaN diode pump laser system

The pump laser system (see Fig. 2 for the full VECSEL system schematic) was built with a multimode, high power InGaN diode laser (Nichia NUBM44, emission aperture width = 107 μm) placed in a temperature-stabilized dedicated mount (Wavelength Electronics MPT-10000, stability <0.008 K over 24h). A low noise current controller (Wavelength Electronics MPL-7500, RMS noise and ripple <20 μA) was used to ensure low intensity noise during pump laser operation, with the facility for an additional external stabilization signal to be implemented if necessary. When operational, a threshold of (0.30 ± 0.01) A was measured with a slope efficiency of (1.51 ± 0.01) W/A, and a maximum output power of 5.2 W when the diode was kept at 10°C. As expected, the diode operation highly depends on the mount temperature: at 28°C the threshold, slope efficiency, and maximum output power change to (0.36 ± 0.01) A, (1.41 ± 0.01) W/A, and 4.1 W, respectively (see Fig. 3(a)). In both cases, a thermal rollover can also be observed for currents above 3.8 A. The high injection current of InGaN diode lasers leads to self-heating mechanisms [39]. These are exacerbated by the relatively poor thermal management in InGaN diode lasers,

Optics EXPRESS

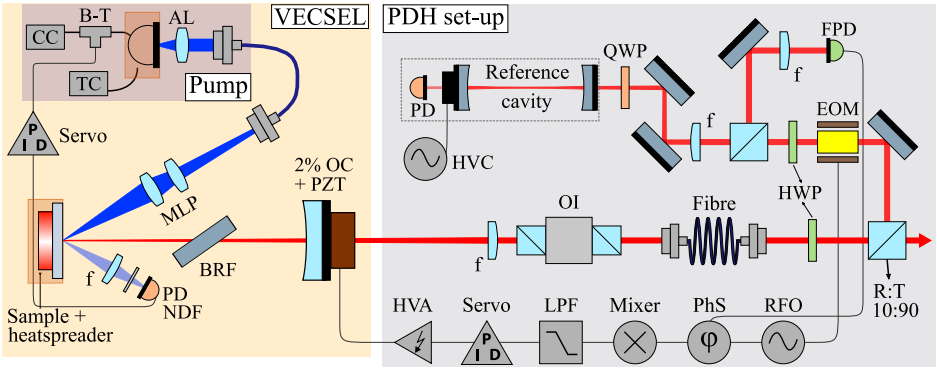

Fig. 2. Full optical system schematics. Left box: compact, diode-pumped, two mirror VECSEL cavity formed by the semiconductor gain mirror and a 2% transmission, plano-concave output coupler (OC). Coarse tuning of the output wavelength is achieved via rotation of an intra-cavity birefringent filter (BRF). The residual reflection of the pump light is captured by a photodetector (PD) after attenuation by a neutral density filter (NDF) and is compared with the reference signal in the servo controller. The correction signal created for pump intensity stabilisation is added to the diode current via a bias-tee (B-T). Right box: After passing through an optical isolator (OI) the VECSEL output is focussed into a single mode fibre for transfer to the setup used for active frequency stabilisation via the Pound-Drever-Hall (PDH) technique, similar to [30]. 10% of the laser output beam is picked off and phase-modulated by an electro-optical modulator (EOM) and coupled to a moderately-high-resolution reference cavity (confocal Fabry-Perot, finesse = 1k and free spectral range = 300 MHz). (The remaining 90% of the output power is available for experiments.) The reflected spectrum is captured by a fast-photodetector (FPD) and is used to create an error signal that is sent back to the laser cavity via a piezo electric transducer (PZT) on which the OC is mounted. CC: current controller; AL: aspheric lens; TC: temperature controller; MLP: matched lens pair; f: lens; HWP: half-wave plate; QWP: quarter-wave plate; HVC: high voltage controller; PhS: phase shifter; RFO: radio-frequency oscillator; LPF: low-pass filter; HVA: high-voltage amplifier.

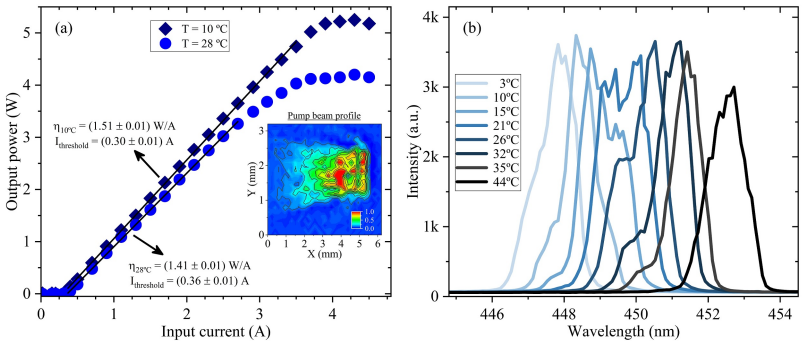

Fig. 3. Characterization of the InGaN diode laser used for optically-pumping the AlGaInP-based VECSEL. The diode laser (Nichia NUBM44) was kept in a temperature-stabilized mount. (a) Diode laser power transfer for two different temperatures: 10°C and 28°C. Inset: beam profile measured before collimation lens was inserted. (b) Emission spectra with increasing mount temperature for a current of 3.5 A.

Optics EXPRESS

related to the use of sapphire substrates that have lower thermal conductivity (≈ 24 $Wm^{-1}K^{-1}$) when compared to GaAs substrates (≈ 46 $Wm^{-1}K^{-1}$) at room temperature [40–42]. Other substrates such as GaN and Si [43] are being investigated to improve the thermal performance of the diode but no device is yet commercially available. There is therefore a high impedance in the path of the heat towards the heatsink during laser operation. As the heat accumulates at the back of the diode packaging, the temperature of the diode increases with time resulting in a reduction in output power levels and device lifetime. In order to minimize the effect of the poor thermal management, the diode thermal contact to its housing was maximized at the back of the mount. The diode has emission at wavelengths between 447 and 453 nm for different temperatures (see Fig. 3(b)) with a spectral width of around 2 nm.

An AR-coated aspheric lens (Thorlabs A230TM-A), with an effective focal length of 4.51 mm and matched numerical aperture of 0.55, was used to collimate the pump beam. The pump beam profile, measured before the collimation lens was inserted, is shown in the inset of Fig. 3(a). In order to improve the beam profile and the optical power distribution, the pump laser is coupled to

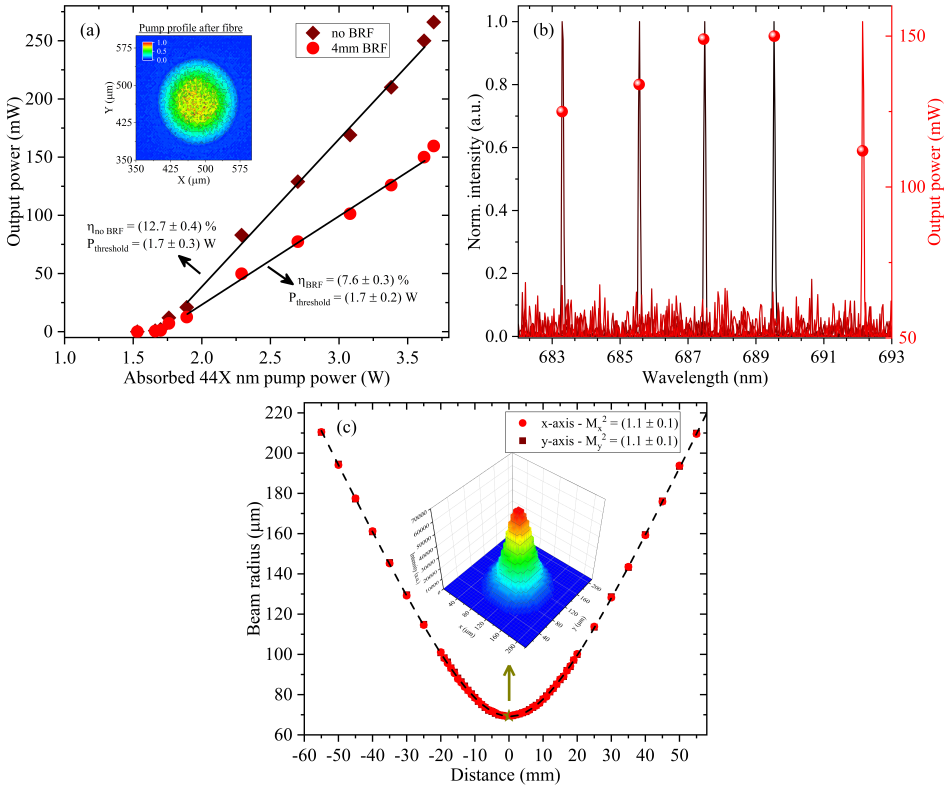

Fig. 4. AlGaInP-based VECSEL characterization under optical pumping at 44X nm and a mount temperature of 22°C. (a) Power transfer without/with the intra-cavity BRF, which presented slope efficiencies of (12.7 ± 0.4) / (7.6 ± 0.3) % and thresholds of (1.7 ± 0.3) / (1.7 ± 0.2) W, respectively. Inset: 44X nm pump beam profile after the multimode optical fiber. (b) Example emission spectra under non-continuous wavelength tuning (lines) with respective output power (circles) of the AlGaInP VECSEL via rotation of the intra-cavity BRF when the sample was pumped with 3.5 W. (c) Single frequency VECSEL beam quality measurement, showing $M^2 = (1.1 \pm 0.1)$ for both x (horizontal) and y axis (vertical). Inset: Beam profile measured at the indicated distance using a commercial CMOS camera (Thorlabs DCC1545M).

Optics EXPRESS

a high power, multimode, 100-µm-core optical fiber (NA = 0.22) with coupling efficiency of 75%. This results in a tophat-like profile (see inset Fig. 4(a)) which is then focused to the gain structure via a matched lens pair (f_1 = 19 mm, f_2 = 25 mm; magnification of 1.32) in a 130-µm-diameter pump spot.

4. VECSEL gain structure characterization

A 4×4 mm^2 piece of the VECSEL gain structure was cleaved from the wafer and the epitaxial surface was capillary-bonded to an uncoated 500-µm-thick, plane-parallel, low birefringence ($\Delta n < 10^{-6}$) synthetic diamond heatspreader [44]. It was placed in a temperature-stabilized brass mount, kept at temperatures between 15 and 25°C via thermo-electric cooling (stability = 0.01 °C). In order to achieve laser oscillation, the bonded gain structure was placed in a linear (two-mirror) cavity, consisting of the sample DBR and a 2% transmission, plano-concave output coupler (Ø = 6 mm, thickness = 3 mm and RoC = 100 mm) mounted on a piezo-electric transducer (PZT) for frequency stabilization purposes. Along with control of the sample temperature for fine tuning of the wavelength with sub-pm precision [16], a 4-mm quartz plate is used as an intra-cavity birefringent filter (BRF) for coarse wavelength tuning (see Fig. 3). The VECSEL cavity has a total length of 99.5 mm with a theoretical mode size of 120 µm at the gain structure, resulting in a cavity fundamental mode size to pump spot size ratio of 0.92.

Figure 4 summarizes the VECSEL sample characterization when the sample was kept at room temperature (22°C). Output power of 270 mW, a slope efficiency of (12.7 ± 0.4) % and a threshold of (1.7 ± 0.3) W were measured without the BRF (see Fig. 4(a)). The insertion of the intra-cavity filter and careful adjustment of the cavity length enabled single frequency operation to be achieved at wavelengths between 682 and 693 nm (see Fig. 4(b)), in a circularly-symmetric single transverse mode (TEM_{00}) with measured $M^2 = (1.1 \pm 0.1)$, see Fig. 4(c). At the target wavelength of 689 nm, output power of 140 mW with a slope efficiency of (7.6 ± 0.3) % and a threshold of (1.7 ± 0.2) W was measured.

5. Linewidth reduction and noise measurements

In order to reduce the pump intensity noise injected into the VECSEL, a simple intensity stabilization setup is implemented where the fraction of the pump light reflected by the uncoated diamond heatspreader is captured by a photodetector (bandwidth = 350 MHz), after attenuation. The photodetector reading is then compared to a reference signal in a servo controller (New Focus LB1005) where a correction signal is created and sent to the current controller via a bias-tee (Mini-Circuits ZX85-12G-S+), inserted to maximize the intensity stabilization bandwidth to 10 MHz, limited by the servo controller. The relative intensity noise (RIN) of the InGaN pump (see Fig. 5) was measured with the intensity stabilization switched on/off (detection bandwidth of 350 MHz). This shows a reduction in the intensity noise by a factor of 12 dB for frequencies below 10 kHz and 15 dB above 1 MHz up to the correction bandwidth of the servo controller (10 MHz), resulting in a pump laser RIN of −105 dBc/Hz. The influence of this reduction in pump RIN on both the frequency and intensity noise of the VECSEL is now presented.

The VECSEL output beam with output power of 140 mW was coupled to the active frequency stabilization setup via an optical fiber with efficiency of 70%. We used the Pound-Drever-Hall technique to stabilize the frequency to a reference Fabry-Perot cavity (finesse = 1k, free spectral range = 300 MHz) to compensate for the influence of environmental noise on the air-spaced laser system and free-standing optical mounts. Figure 2 depicts the full optical system where 10% of the output power is picked off and modulated by an electro-optical modulator (phase modulator EOM, frequency modulation = 74 MHz, RF power <20 dBm, input impedance = 1 MΩ). The correction signal is created from the demodulation of the reference cavity reflected spectra, captured by a fast-photodetector, and is then sent back to the laser cavity PZT via a servo

Optics EXPRESS

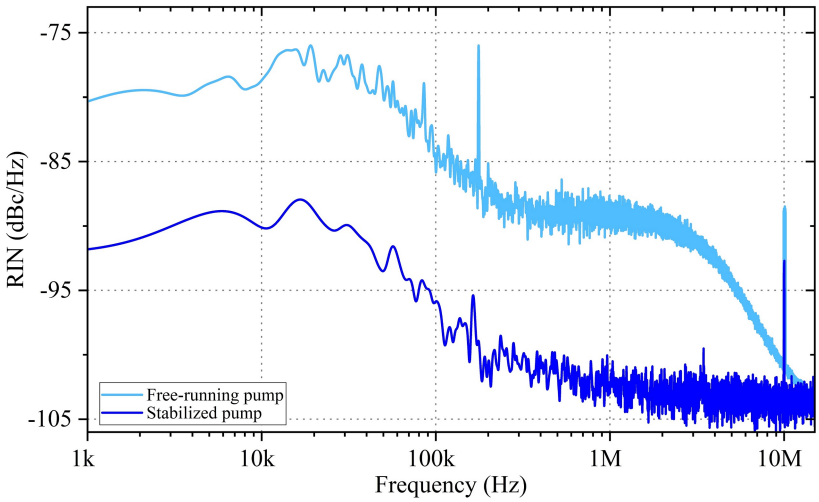

Fig. 5. InGaN pump laser system relative intensity noise; with (blue) and without (light blue) intensity stabilization.

controller (Vescent Photonics D2-125). The correction bandwidth of the frequency stabilization setup is 30 kHz [30].

The VECSEL system performance was characterized in intensity and frequency noise. The relative intensity noise of the VECSEL system was measured three times under increasing degrees of active stabilization (see Fig. 6): (1) free-running pump and VECSEL, (2) free-running pump and frequency-locked VECSEL, and (3) intensity-stabilized pump and frequency-locked VECSEL. Here, the simple pump intensity stabilization resulted in a further VECSEL RIN reduction at all frequencies up to 1 MHz and a reduction of >25 dB for frequencies below 10 kHz. The VECSEL RIN is <−130 dBc/Hz for all frequencies above 100 kHz and <−142 dBc/Hz for frequencies above 2 MHz. Peaks are noticeable for frequencies above 30 kHz which might be related to mechanical and electronic noise not suppressed by the stabilization techniques implemented here.

A frequency noise power spectrum density (FNPSD) is calculated via the residual (AC) error signal generated by the servo controller recorded over acquisition times of 2s. This was carried out for the same three stabilization conditions (see Fig. 7(a)). The signal recorded for (1) has a RMS noise of 75 kHz and presents VECSEL, environmental, and pump-related FNPSD contributions for frequencies between 1 Hz and 1.5 MHz, limited by the acquisition time and detection bandwidth respectively. In (2), a RMS noise of 2.1 kHz is observed with the signal baseline reduced but with peaks below 1 kHz and above 40 kHz dominating the spectrum. It is important to highlight here that the high finesse external cavity acts as a low pass filter which attenuates high frequency fluctuations with a 3-dB cutoff frequency given by $f_{cutoff,3dB} = \nu_{FSR}/2F$, where ν_{FSR} is the cavity free spectral range and F its finesse [45]. For the VECSEL cavity presented here, any pump intensity noise below the cutoff frequency of ~2.4 MHz (beyond the range of our detection bandwidth for the FNPSD measurement) will have an impact in the overall noise performance of the laser and its linewidth. Although efficient temperature stabilization and the low noise current controller help to minimize the noise levels of the diode laser, intensity noise still plays a major role in the overall laser performance. In this scenario, the intensity stabilization applied to the InGaN diode is necessary to reduce the VECSEL frequency noise below the laser cavity cutoff.

Optics EXPRESS

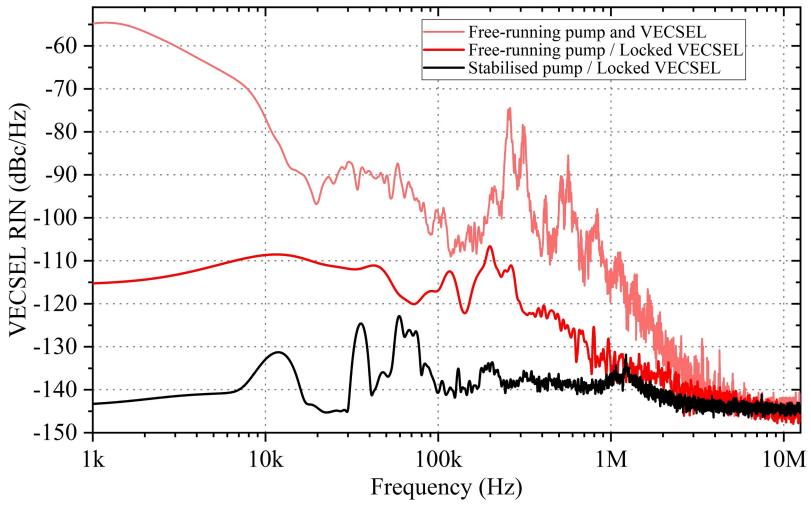

Fig. 6. Relative intensity noise of the AlGaInP VECSEL when optically-pumped with an InGaN laser diode for three modes of active stabilization: (pink) free-running pump and VECSEL, (red) free-running pump and frequency-locked VECSEL, and (black) intensity-stabilized pump and frequency-locked VECSEL. The shot noise limit is −161 dB/Hz.

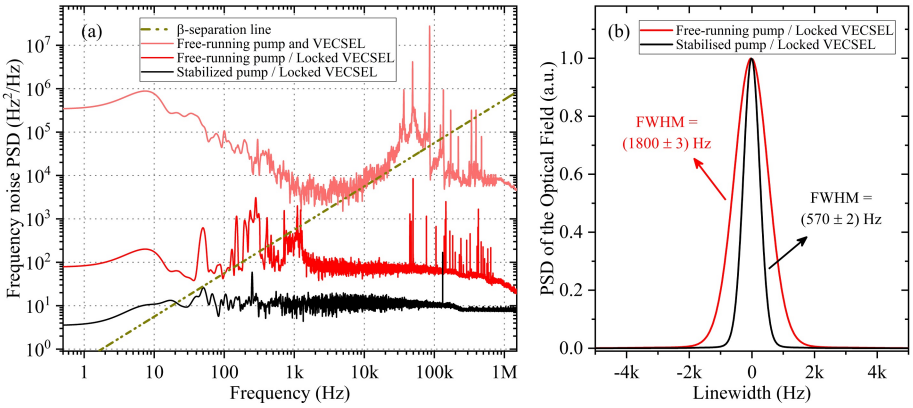

Fig. 7. (a) Frequency noise power spectral density of the AlGaInP-based VECSEL when pumped with the InGaN diode laser for three modes of active stabilization: (pink) free-running pump and VECSEL, (red) free-running pump and frequency-locked VECSEL, and (black) intensity-stabilized pump and frequency-locked VECSEL. The β-separation line (dash dotted line) is also plotted, dividing the graph into two regions with low and high frequency modulation which contributes to the central and wings of the laser line-shape, respectively. (b) Power spectral density of the optical field of the locked VECSEL, reconstructed via autocorrelation and the Wiener-Khintchine theorem from the spectra presented in (a) for the locked VECSEL; with (black), and without (red) intensity stabilization. A linewidth of (1800 ± 3) Hz is reduced to (570 ± 2) Hz when intensity stabilization is applied

Optics EXPRESS

When the pump stabilization is switched on (see Fig. 7(a)), further reduction in the FNPSD in different frequency bands can be observed, reducing the peaks located at frequencies <1 kHz and >40 kHz. These peaks are originated in intensity noise injected by the pump laser into the VECSEL up to the laser cavity frequency cut-off. The remaining peaks are at frequency bands related to pure and thermally-induced mechanical noise caused mainly by environmental influences and the high frequency noisè band is caused by additional electronics noise.

Figure 7(a) also shows the β-separation line, defined as $S_\beta(f) = 8(\ln 2)f/\pi^2$ [46], where f represents the Fourier frequencies, which divides the PSD graph into two regions: frequency noise above the separation line, which directly affects the linewidth; and below it, which contributes only to the wings of the line shape. For the VECSEL performance depicted here it is clear that the reduction of intensity noise in the pump laser system is crucial to further improve the laser linewidth. The linewidth was estimated by reconstructing the shape of the optical field via auto-correlation and the Wiener-Khintchine theorem using the power spectral density data [46]. Using this technique, which estimates laser linewidth relative to a suitable reference cavity, linewidths of (1800 ± 3) Hz and (570 ± 2) Hz (see Fig. 7(b)) are calculated for the central (or Gaussian) part of the emission spectra when the pump intensity stabilization is switched off and on, respectively. When both the VECSEL and pump are free-running, a linewidth of 150 kHz is estimated.

6. Conclusions

We have reported the design, growth, characterization and improved performance in output power, stability and noise performance of an AlGaInP-VECSEL gain structure pumped by a high power InGaN diode laser. Although extensively implemented in VECSELs with direct emission at near and mid-IR wavelengths (using 808 nm bars), diode-pumping at visible wavelengths is more challenging, not only due to the relative lack of commercially-available high power devices, but in this case also the necessary re-design of the gain structures to adapt to the short absorption length of the available pump wavelengths. AlGaInP-based VECSELs have previously been barrier- [17] and in-well-pumped [20] at green and red wavelengths, respectively, using bulky laser systems based on second-harmonic generation from IR emitters, recently reaching unprecedented ultra-narrow linewidths [30]. In this work we have significantly reduced the size, weight, power and costs (SWaP-C) of an AlGaInP VECSEL system while maintaining high brightness and sub-kHz linewidth, replacing the green pump laser with an inexpensive InGaN pump diode with emission at blue wavelengths (44X–45X nm). Using a redesigned gain structure with an asymmetric distribution of compressively-strained GaInP quantum wells within a short gain region, we achieved high brightness with emission wavelength between 678 and 693 nm, tunable via an intra-cavity birefringent filter, when pumped with the InGaN diode laser. Single frequency operation at 689 nm with >140 mW output power and linewidth (1800 ± 3) Hz was demonstrated when the VECSEL cavity was frequency-stabilized to a commercial air-spaced Fabry-Perot cavity via the Pound-Drever-Hall technique. To reduce the influence of intensity noise transferred to the VECSEL cavity from the pump laser, a simple intensity-stabilization circuit was implemented, resulting in a linewidth of (570 ± 2) Hz with a relative intensity noise <-120 dBc/Hz for all frequencies >1 Hz. This work represents a significant step towards a more compact visible VECSEL system with a fully integrated pump laser while maintaining the same high performance in terms of output power, ultra-narrow linewidth and overall stability required for next generation cold-atom-based quantum technologies.

Funding. Engineering and Physical Sciences Research Council (EP/I022791/1, EP/M013294/1, EP/T001046/1).

Acknowledgment. Data related to this publication have been made available at the University of Strathclyde data repository [47].

Disclosures. The authors declare no conflicts of interest.

Optics EXPRESS

References

1. N. Kolachevsky, P. Fendel, S. G. Karshenboim, and T. W. Hansch, "2S hyperfine structure of atomic deuterium," Phys. Rev. A **70**(6), 062503 (2004).
2. H. S. Margolis, G. P. Barwood, G. Huang, H. A. Klein, S. N. Lea, K. Szymaniec, and P. Gill, "Hertz-level measurement of the optical clock frequency in a single ^{88}Sr+ ion," Science **306**(5700), 1355–1358 (2004).
3. M. Takamoto, F. L. Hong, R. Higashi, and H. Katori, "An optical lattice clock," Nature **435**(7040), 321–324 (2005).
4. S. Falke, N. Lemke, C. Grebing, B. Lipphardt, S. Weyers, V. Gerginov, N. Huntemann, C. Hagemann, A. Al-Masoudi, S. Häfner, S. Vogt, U. Sterr, and C. Lisdat, "A strontium lattice clock with 3×10^{-17} inaccuracy and its frequency," New J. Phys. **16**(7), 073023 (2014).
5. M. Kuznetsov, F. Hakimi, R. Sprague, and A. Mooradian, "High-power (>0.5-W CW) diode-pumped vertical-external-cavity surface-emitting semiconductor lasers with circular TEM_{00} beams," IEEE Photonics Technol. Lett. **9**(8), 1063–1065 (1997).
6. M. Guina, A. Rantamki, and A. Hrkönen, "Optically pumped VECSELs: review of technology and progress," J. Phys. D: Appl. Phys. **50**(38), 383001 (2017).
7. B. Cocquelin, D. Holleville, G. Lucas-Leclin, I. Sagnes, A. Garnache, M. Myara, and P. Georges, "Tunable single-frequency operation of a diode-pumped vertical external-cavity laser at the cesium D-2 line," Appl. Phys. B **95**(2), 315–321 (2009).
8. D. Paboeuf, P. J. Schlosser, and J. E. Hastie, "Frequency stabilization of an ultraviolet semiconductor disk laser," Opt. Lett. **38**(10), 1736–1738 (2013).
9. E. Kantola, T. Leinonen, S. Ranta, M. Tavast, and M. Guina, "High-efficiency 20 W yellow VECSEL," Opt. Express **22**(6), 6372–6380 (2014).
10. F. Zhang, B. Heinen, M. Wichmann, C. Moller, B. Kunert, A. Rahimi-Iman, W. Stolz, and M. Koch, "A 23-watt single-frequency vertical-external-cavity surface-emitting laser," Opt. Express **22**(11), 12817–12822 (2014).
11. H. Kahle, K. Nechay, J.-P. Pentinnen, A. Tukiainen, S. Ranta, and M. Guina, "AlGaAs-based vertical-external-cavity surface-emitting laser exceeding 4 W of direct emission power in the 740-790 nm spectral range," Opt. Lett. **43**(7), 1578–1581 (2018).
12. Y. Kaneda, M. Hart, S. H. Warner, J.-P. Penttinen, and M. Guina, "Narrow-linewidth operation of folded 1178nm VECSEL with twisted-mode cavity," Opt. Express **27**(19), 27267–27272 (2019).
13. S. Denet, B. Chomet, V. Lecocq, L. Ferrieres, M. Myara, L. Cerutti, I. Sagnes, and A. Garnache, "Industrial integration of high coherence tunable VECSEL in the NIR & MIR," SPIE LASE - VECSELs VI **9734**, 97340C (2016).
14. B. Cocquelin, G. Lucas-Leclin, P. Georges, I. Sagnes, and A. Garnache, "Design of a low-threshold VECSEL emitting at 852 nm for Cesium atomic clocks," Opt. Quantum Electron. **40**(2-4), 167–173 (2008).
15. T. Wunderer, J. E. Northrup, Z. Yang, M. Teepe, A. Strittmatter, N. M. Johnson, P. Rotella, and M. Wraback, "In-well pumping of InGaN/GaN vertical-external-cavity surface-emitting lasers," Appl. Phys. Express **99**(20), 201109 (2011).
16. D. Paboeuf and J. E. Hastie, "Tunable narrow linewidth AlGaInP semiconductor disk laser for Sr atom cooling applications," Appl. Opt. **55**(19), 4980–4984 (2016).
17. J. E. Hastie, S. Calvez, M. D. Dawson, T. Leinonen, A. Laakso, J. Lyytikinen, and M. Pessa, "High power CW red VECSEL with linearly polarized TEM_{00} output beam," Opt. Express **13**(1), 77–81 (2005).
18. K. Nechay, H. Kahle, J.-P. Pentinnen, P. Rajala, A. Tukiainen, S. Ranta, and M. Guina, "AlGaAs/AlGaInP VECSELs With Direct Emission at 740–770 nm," IEEE Photonics Technol. Lett. **31**(15), 1245–1248 (2019).
19. H.-M. Phung, H. Kahle, J.-P. Penttinen, P. Rajala, S. Ranta, and M. Guina, "Power scaling and thermal lensing in 825 nm emitting membrane external-cavity surface-emitting lasers," Opt. Lett. **45**(2), 547–550 (2020).
20. C. M. N. Mateo, U. Brauch, T. Schwarzbäck, H. Kahle, M. Jetter, M. A. Ahmed, P. Michler, and T. Graf, "Enhanced efficiency of AlGaInP disk laser by in-well pumping," Opt. Express **23**(3), 2472–2486 (2015).
21. S. Nakamura, "InGaN-based blue/green LEDs and laser diodes," Adv. Mater. **8**(8), 689–692 (1996).
22. A. Smith, J. E. Hastie, H. D. Foreman, T. Leinonen, M. Guina, and M. D. Dawson, "GaN diode-pumping of red semiconductor disk laser," Electron. Lett. **44**(20), 1195–1196 (2008).
23. M. Schubert, J. A. Woollam, G. Leibiger, B. Rheinlander, I. Pietzonka, T. Sass, and V. Gottschalch, "Isotropic dielectric functions of highly disordered $Al_xGa_{1-x}InP$ ($0\leq x\leq 1$) lattice matched to GaAs," J. Appl. Phys. **86**(4), 2025–2033 (1999).
24. S. Turcotte and M. Daraselia, "Generalized model of the dielectric function of AlInGaP alloys," J. Appl. Phys. **113**(9), 093103 (2013).
25. M. Y. A. Raja, S. R. J. Brueck, M. Osinski, C. F. Schaus, J. G. Mcinerney, T. M. Brennan, and B. E. Hammons, "Resonant Periodic Gain Surface-Emitting Semiconductor-Lasers," IEEE J. Quantum Electron. **25**(6), 1500–1512 (1989).
26. H. Wang, Y. Kawahito, R. Yoshida, Y. Nakashima, and K. Shiokawa, "Development of a high-power blue laser (445 nm) for material processing," Opt. Lett. **42**(12), 2251–2254 (2017).
27. T. C. Wu, Y. C. Chi, H. Y. Wang, C. T. Tsai, and G. R. Lin, "Blue Laser Diode Enables Underwater Communication at 12.4 Gbps," Sci. Rep. **7**(1), 40480 (2017).
28. S. P. DenBaars, D. Feezell, K. Kelchner, S. Pimputkar, C. C. Pan, C. C. Yen, S. Tanaka, Y. J. Zhao, N. Pfaff, R. Farrell, M. Iza, S. Keller, U. Mishra, J. S. Speck, and S. Nakamura, "Development of gallium-nitride-based light-emitting diodes (LEDs) and laser diodes for energy-efficient lighting and displays," Acta Mater. **61**(3), 945–951 (2013).

Optics EXPRESS

29. S. Masui, Y. Nakatsu, D. Kasahara, and S.-I. Nagahama, *Recent improvement in nitride lasers, SPIE OPTO* (SPIE, 2017), Vol. 10104.
30. P. H. Moriya, Y. Singh, K. Bongs, and J. E. Hastie, "Sub-kHz-linewidth VECSELs for cold atom experiments," Opt. Express **28**(11), 15943–15953 (2020).
31. G. Baili, M. Alouini, D. Dolfi, F. Bretenaker, I. Sagnes, and A. Garnache, "Shot-noise-limited operation of a monomode high-cavity-finesse semiconductor laser for microwave photonics applications," Opt. Lett. **32**(6), 650–652 (2007).
32. M. Myara, M. Sellahi, A. Laurain, A. Garnache, A. Michon, and I. Sagnes, "Noise Properties of NIR and MIR VECSELs," *2013 22nd International Conference on Noise and Fluctuations (ICNF)* (2013).
33. S. De, G. Baili, M. Alouini, J.-C. Harmand, S. Bouchoule, and F. Bretenaker, "Class-A dual-frequency VECSEL at telecom wavelength," Opt. Lett. **39**(19), 5586–5589 (2014).
34. A. L. Schawlow and C. H. Townes, "Infrared and Optical Masers," Phys. Rev. **112**(6), 1940–1949 (1958).
35. C. H. Henry, "Theory of the Linewidth of Semiconductor-Lasers," IEEE J. Quantum Electron. **18**(2), 259–264 (1982).
36. T. Yokotsuka, A. Takamori, and M. Nakajima, "Growth of heavily Be-doped AlInP by gas source molecular beam epitaxy," Appl. Phys. Express **58**(14), 1521–1523 (1991).
37. D. P. Bour, R. S. Geels, D. W. Treat, T. L. Paoli, F. Ponce, R. L. Thornton, B. S. Krusor, R. D. Bringans, and D. F. Welch, "Strained $Ga_xIn_{1-x}P/(AlGa)_{0.5}In_{0.5}P$ heterostructures and quantum-well laser diodes," IEEE J. Quantum Electron. **30**(2), 593–607 (1994).
38. N. Yamada, G. Roos, and J. S. H. Jr, "Threshold reduction in strained InGaAs single quantum well lasers by rapid thermal annealing," Appl. Phys. Lett. **59**(9), 1040–1042 (1991).
39. J. Dallas, G. Pavlidis, B. Chatterjee, J. S. Lundh, M. Ji, J. Kim, T. Kao, T. Detchprohm, R. D. Dupuis, S. Shen, S. Graham, and S. Choi, "Thermal characterization of gallium nitride p-i-n diodes," Appl. Phys. Lett. **112**(7), 073503 (2018).
40. S. Nakamura, M. Senoh, S. Nagahama, N. Iwasa, T. Yamada, T. Matsushita, Y. Sugimoto, and H. Kiyoku, "Continuous-wave operation of InGaN multi-quantum-well-structure laser diodes at 233 K," Appl. Phys. Express **69**(20), 3034–3036 (1996).
41. M. Steube, K. Reimann, D. Frohlich, and S. J. Clarke, "Free excitons with n=2 in bulk GaN," Appl. Phys. Express **71**, 948–949 (1997).
42. M. Kawaguchi, O. Imafuji, S. Nozaki, H. Hagino, K. Nakamura, S. Takigawa, T. Katayama, and T. Tanaka, "Record-breaking high-power InGaN-based laser-diodes using novel thick-waveguide structure," in *2016 International Semiconductor Laser Conference (ISLC)*, 2016), 1–2.
43. Y. Sun, K. Zhou, M. Feng, Z. Li, Y. Zhou, Q. Sun, J. Liu, L. Zhang, D. Li, X. Sun, D. Li, S. Zhang, M. Ikeda, and H. Yang, "Room-temperature continuous-wave electrically pumped InGaN/GaN quantum well blue laser diode directly grown on Si," Light: Sci. Appl. **7**(1), 13 (2018).
44. A. J. Kemp, G. J. Valentine, J. Hopkins, J. E. Hastie, S. A. Smith, S. Calvez, M. D. Dawson, and D. Burns, "Thermal management in vertical-external-cavity surface-emitting lasers: finite-element analysis of a heatspreader approach," IEEE J. Quantum Electron. **41**(2), 148–155 (2005).
45. N. Uehara and K. Ueda, "Accurate measurement of ultralow loss in a high-finesse Fabry-Perot interferometer using the frequency response functions," Appl. Phys. B **61**(1), 9–15 (1995).
46. G. Di Domenico, S. Schilt, and P. Thomann, "Simple approach to the relation between laser frequency noise and laser line shape," Appl. Opt. **49**(25), 4801–4807 (2010).
47. P. H. Moriya, "Data for: InGaN-diode-pumped AlGaInP VECSEL with sub-kHz linewidth at 689 nm," University of Strathclyde (2020).